



Preparation of CuO nanoparticles by thermal decomposition of double-helical dinuclear copper(II) Schiff-base complexes

Aliakbar Dehno Khalaji^{1,2*} and Debasis Das³

1. Department of Chemistry, Faculty of Science, Golestan University, Gorgan, Iran

2. Cubane Chemistry of Hircane Co., Gorgan, Iran

3. Department of Chemistry, University of Burdwan, Burdwan, West Bangal, India

Received 1 June 2015; Accepted 12 January 2016

* Corresponding author Email: alidkhalaji@yahoo.com & ad.khalaji@gu.ac.ir

Abstract

In this paper, two double-helical dinuclear copper(II) complexes of bis-N,O-bidentate Schiff-base ligands bis (3-methoxy-N-salicylidene-4,4'-diaminodiphenyl) sulfone (L^1) and bis(5-bromo-N-salicylidene-4,4'-diaminodiphenyl)sulfone (L^2) were prepared and characterized by elemental analyses (CHN), as well as thermal analysis. Elemental analyses (CHN) suggested that the reaction between ligands and copper salt has occurred in 1:1 molar ratio. In these complexes, the Schiff-base ligands behave as anionic and bis-bidentate chelate and are coordinated with the copper (II) ion via two phenolic oxygen and two iminic nitrogen atoms. In these double-helical dinuclear complexes, each copper (II) center has a pseudo-tetrahedral coordination sphere two-wrapped ligand. Thermal analysis of ligands and their complexes were studied in the range of room temperature to 750°C with a heating rate of 10°C min⁻¹. TG plots show that the ligands and their complexes are thermally decomposed via 2 and 3 thermal steps, respectively. In addition, the complexes thermally decomposed in air at 520°C for 3 h. The obtained solids were characterized by Fourier Transform Infrared Spectroscopy (FT-IR), X-ray Powder Diffraction (XRD), and Transmission Electron Microscopy (TEM). The X-ray pattern result shows that the CuO nanoparticles are pure and single phase. The TEM result shows the prepared CuO nanoparticles were very small and similar shape with particle size about <50 nm. On the basis of the above results, this method is therefore potentially capable of forming other transition metal oxide nanoparticles.

Keywords: CuO nanoparticles, decomposed, double-helical dinuclear copper (II) complexes, pseudo-tetrahedral, thermal analysis.

1. Introduction

Di and tetranuclear copper (II) complexes with bis-bidentate N,O Schiff-base ligands have become relatively common in the coordination chemistry [1-8]. They have been much interested for the study of the supramolecular

chemistry [1-8]. After Lehn and co-workers introduced the term of helicate in 1987, large numbers of helical structures have been described [1-9]. Youshida and co-workers reported di- and tetranuclear copper (II)

complexes with bis-bidentate N, O Schiff-base ligands that X-ray crystallography revealed that the final structure (di- or tetranuclear double-helical) is greatly controlled by the $\pi\pi$ and CH $\cdot\pi$ interaction of Schiff-base ligands [5]. Thermal studies provide useful information such as the metal-ligand bonds and the presence of crystallization and/or coordination water in transition metal Schiff-

base complexes [10-15]. As a part of our ongoing work, dealing with the thermal studies on Schiff-base complexes [16-20], in this paper, we studied the thermal decomposition of double-helical dinuclear copper (II) complexes [3-5] (Fig. 1). Also, we prepared CuO nanoparticles using solid-state thermal decomposition at 500°C.

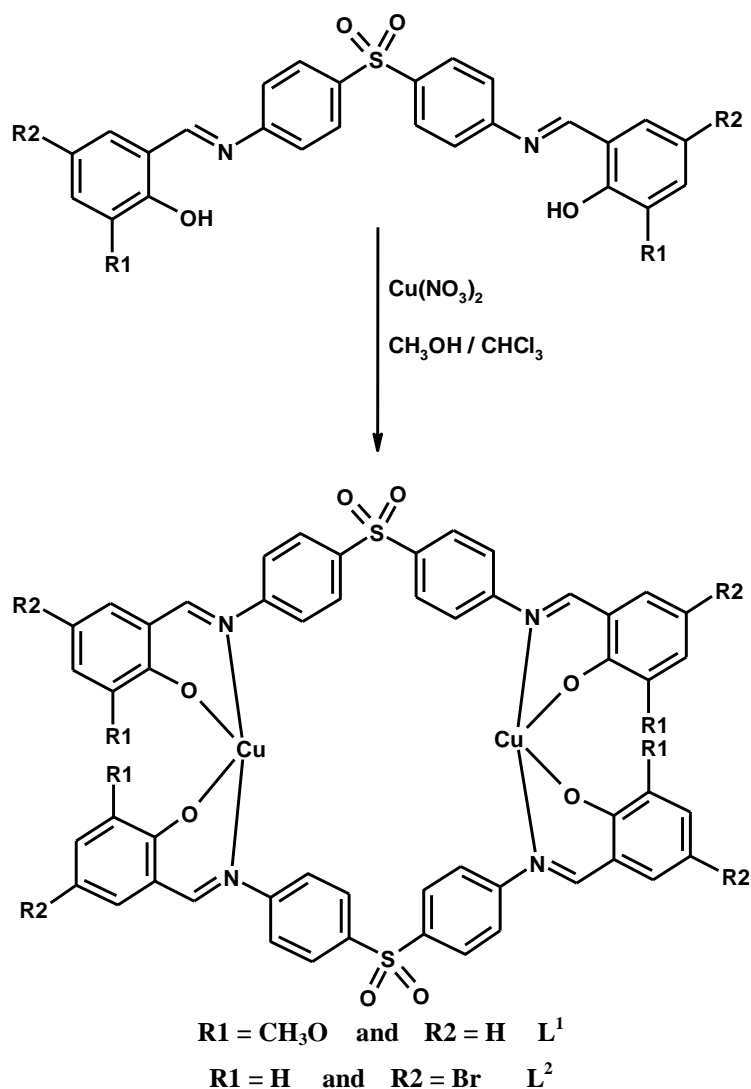


Fig. 1. The chemical structures of bis-N,O-bidentate Schiff-base ligands and their double-helical dinuclear copper(II) complexes

2. Experiments

2.1. Materials and Instruments

Methanol, chloroform, 3-methoxysalicylaldehyde, 5-bromosalicylaldehyde, bis(4-aminophenyl)sulfone, and $\text{Cu}(\text{NO}_3)_2 \cdot 3\text{H}_2\text{O}$ have been purchased from Merck and used as received.

Infrared spectra are recorded using KBr disk on a FT-IR (Perkin-Elmer) spectrometer. Elemental analyses are carried out using a Heraeus CHN-O-Rapid analyzer. The TG are performed on a Perkin Elmer TG/DTA lab system 1 (Technology by SII) in nitrogen atmosphere with a heating rate of 20°C/min in the temperature

span of 30–750°C. X-ray powder diffraction (XRD) patterns were performed using Philips X'pert diffractometer with monochromatic CuK α radiation. The transmission electron microscopy (TEM) images were obtained from a JEOL JEM 1400 transmission electron microscope with an accelerating voltage of 120 kV.

2.2. Preparation of Schiff-base ligands

Bis-N, O-bidentate Schiff-base ligands bis (3-methoxy-N-salicylidene-4, 4'-diaminodiphenyl) sulfone (L^1), bis (5-bromo-N-salicylidene-4, 4'-diaminodiphenyl) sulfone (L^2) were prepared using the reported procedure [3-6]. *Anal.* calcd for L^1 , C₂₈H₂₄N₂O₆S: C, 65.12; H, 4.65, N, 5.43 and S, 6.20%; Found C, 65.16; H, 4.69, N, 5.47 and S, 6.23%.

2.3. Preparation of double-helical dinuclear copper (II) complexes

The preparation of two double-helical dinuclear copper (II) complexes [Cu₂(L^1)₂] and [Cu₂(L^2)₂] is identical, and the synthetic process is the following: to a solution of ligand L^1 (0.052 g, 1 mmol) or L^2 (0.062 g, 1 mmol) in chloroform (10 mL) was added a methanol solution (10 mL) of Cu(NO₃)₂·3H₂O (0.026 g, 1 mmol). The solution became dark brown immediately. The resulting solution was refluxed for 2h and then cooled to room temperature. Slow evaporation of solvent for few days gives the microcrystalline powders of the complexes. *Anal.* calcd for [Cu₂(L^1)₂], C₅₆H₄₄N₄Cu₂O₁₂S₂: C, 58.18; H, 3.81, N, 4.85

and S, 5.54%; Found C, 58.11; H, 3.85, N, 4.77 and S, 5.53%. *Anal.* calcd for [Cu₂(L^2)₂], C₅₂H₃₂N₄Cu₂O₈Br₄S₂: C, 46.19; H, 2.37; N, 4.14 and S, 4.74%; Found C, 46.16; H, 2.29; N, 4.20 and S, 4.69%.

2.4. Preparation of CuO nanoparticles

Dark brown microcrystalline powder of the double-helical dinuclear copper (II) complexes (~0.5 g) was loaded on a platinum crucible and placed in an electrical furnace, and heated at a rate of 10°C/min in air up to 520°C. After 3 h, the resulting nanoparticles were washed thrice with ethanol to remove any eventual impurities, and allowed to dry in air for 2 days. FT-IR (KBr pellet, cm⁻¹): 523 cm⁻¹ for nanoparticles prepared from [Cu₂(L^1)₂] and 518 cm⁻¹ for nanoparticles prepared from [Cu₂(L^2)₂].

3. Results and Discussion

3.1. Thermal analysis of the Schiff-base ligands and their complexes

Thermal behaviour (TGA) of the bis-N,O-bidentate Schiff-base ligands (Fig. 2) and their double-helical dinuclear copper(II) complexes (Fig. 3) has been studied under N₂ atmosphere from room temperature to 750 °C with the heating rate of 20°C per minute. Figures 2 and 3 show there is no mass loss up to ~ 249°C for L^1 , 213°C for L^2 , 241°C for [Cu₂(L^1)₂] and 260°C for [Cu₂(L^2)₂], confirming the absence of any crystalline water (solvent) molecules in the ligands and their complexes.

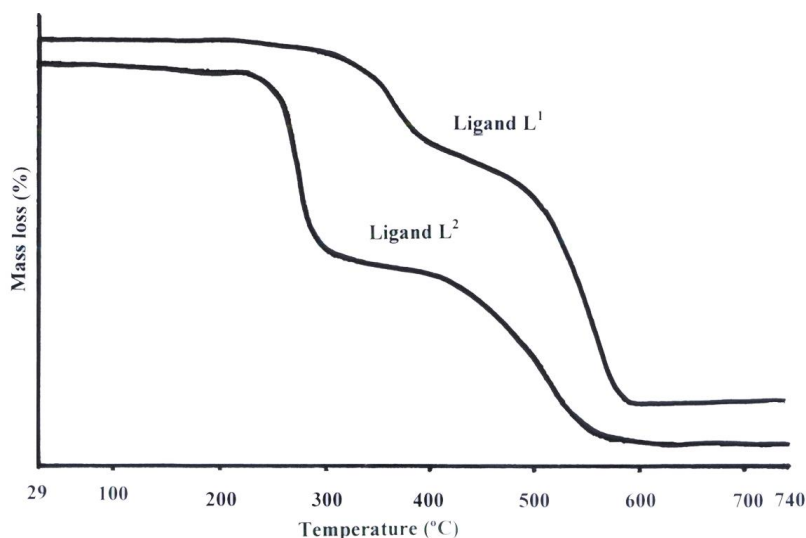


Fig. 2. The TGA curves of free bis-N,O-bidentate Schiff base ligands

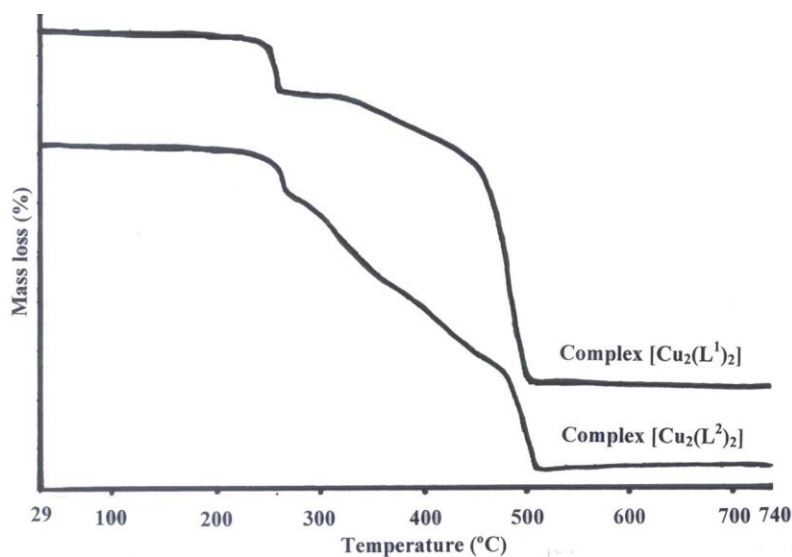


Fig. 3. The TGA curves of double-helical dinuclear copper(II) complexes

The N,O-bidentate Schiff-base ligands \mathbf{L}^1 and \mathbf{L}^2 lose $\approx 99\%$ of their weight via two thermal stages. In the first stage, ligand \mathbf{L}^1 shows a mass loss of 29.37% in the temperature range 248–389°C, while \mathbf{L}^2 shows a mass loss of 56.12% in the temperature range 213–336°C. In the second stage, ligand \mathbf{L}^1 shows a mass loss of 69.94% in the temperature range 389–598°C, while \mathbf{L}^2 shows a mass loss of 43.08% in the temperature range 336–621°C. The final product may be residual carbon.

The double-helical dinuclear copper(II) complex $[\text{Cu}_2(\mathbf{L}^1)_2]$ loses $\approx 86.5\%$ of its weight and $[\text{Cu}_2(\mathbf{L}^2)_2]$ loses $\approx 88\%$ of its weight via three thermal stages. In the first to third stages, complex $[\text{Cu}_2(\mathbf{L}^1)_2]$ shows mass loss of 10.27% in the temperature range 241–254°C, 21.44% in the temperature range 254–451°C, and 55.25% in the temperature range 451–515°C. It is suggested that final residue content in thermal decomposition of $[\text{Cu}_2(\mathbf{L}^1)_2]$ is 2CuO according to overall mass loss (exp. 13.04%, calcd. 13.77%). While, in the first to third stages, complex $[\text{Cu}_2(\mathbf{L}^2)_2]$ shows mass loss of 9.43% in the temperature range 259–267°C, 50.53% in the temperature range 267–478°C, and 28.47% in the temperature range 478–510°C. It is suggested that final residue content in thermal decomposition of $[\text{Cu}_2(\mathbf{L}^2)_2]$ is 2CuO according to overall mass loss and residual

carbon (exp. 11.57%, calcd. 11.76%). Based on the thermal analysis, CuO can be prepared by calcining the double-helical dinuclear copper(II) complexes $[\text{Cu}_2(\mathbf{L}^1)_2]$ and $[\text{Cu}_2(\mathbf{L}^2)_2]$ as precursors at $\approx 520^\circ\text{C}$. Therefore, the choice of suitable calcinations temperature is highly dependent on the results of thermal analysis.

3.2. Characterization of prepared CuO nanoparticles

The double-helical dinuclear copper(II) complexes $[\text{Cu}_2(\mathbf{L}^1)_2]$ and $[\text{Cu}_2(\mathbf{L}^2)_2]$ are thermally decomposed in solid state at 520°C for 3 h. The final residue content is CuO nanoparticles and is characterized by FT-IR spectroscopy, XRD and TEM. Figure 4 shows FT-IR spectra of CuO nanoparticles obtained from solid-state thermal decomposition of complexes at 520°C . The samples show absorption maxima at 523 cm^{-1} for nanoparticles prepared from $[\text{Cu}_2(\mathbf{L}^1)_2]$ and at 518 cm^{-1} for nanoparticles prepared from $[\text{Cu}_2(\mathbf{L}^2)_2]$ which are due to Cu-O stretching mode [21–23], while for bulk CuO, vibrational frequency of Cu-O is found at $\approx 450\text{ cm}^{-1}$ [21, 24]. The blue-shift of the vibrational frequency of Cu-O nanoparticles can be attributed to the small size. Also two broad bands appeared at 3450 and 1645 cm^{-1} corresponding to the stretching modes of the hydroxyls of adsorbed water molecules [21, 24].

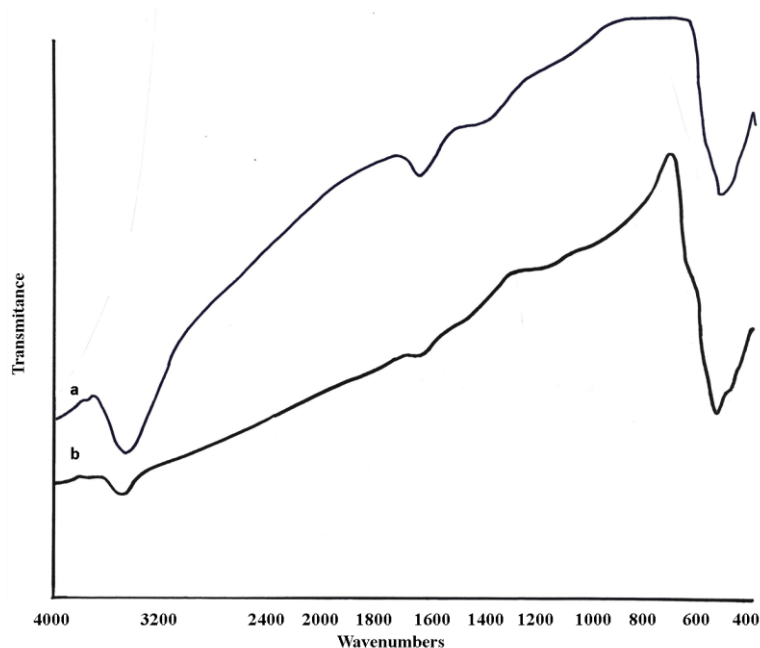


Fig. 4. FT-IR spectra of CuO nanoparticles prepared from $[\text{Cu}_2(\text{L}^1)_2]$ (a) and $[\text{Cu}_2(\text{L}^2)_2]$ (b)

Figure 5 represents the XRD pattern ($2\theta < 70^\circ$) of the obtained CuO products calcined at 520°C . All the diffraction peaks could be indexed to crystalline monoclinic structure, compared with the data of the JCPDS File No.45-0937, and indicating the formation of single phase CuO [21-23, 25-29]. No other peak is observed belonging to any impurity such as Cu, Cu_2O indicating the high purity of CuO nanoparticles. The peaks at about 2θ values of 33° , 36° , 39° , 48° , 54° , 58° ,

62° , 66° , 67° , and 69° are assigned to the (110), (002), (111), (202), (020), (202), (113), (311), (311), and (220) crystal planes, respectively [23, 26]. The crystalline size of the CuO nanoparticles based on X-ray peak broadening were determined using the Debye-Scherrer equation $d (\text{\AA}) = 0.9 \lambda / \beta \cos\theta$. The calculated values are about 35 nm for CuO nanoparticles prepared from $[\text{Cu}_2(\text{L}^1)_2]$ and $[\text{Cu}_2(\text{L}^2)_2]$.

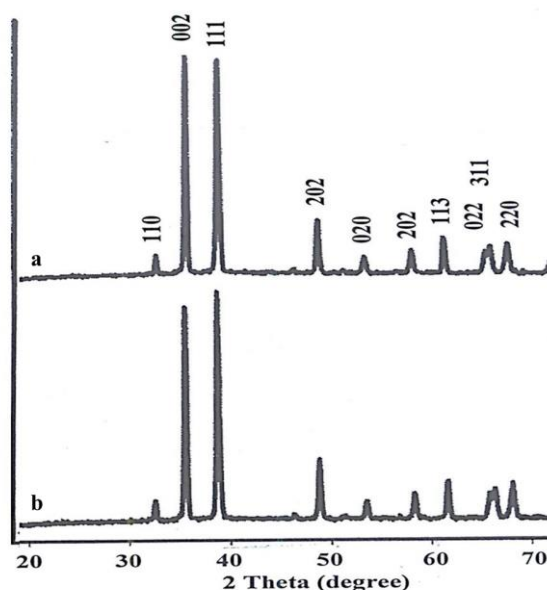


Fig. 5. XRD patterns of CuO nanoparticles prepared from $[\text{Cu}_2(\text{L}^1)_2]$ (a) and $[\text{Cu}_2(\text{L}^2)_2]$ (b)

In addition, the microstructure of the CuO nanoparticles has been examined using TEM (Fig. 6). The TEM samples were prepared by dispersing the powder in ethanol by ultrasonic vibration. The CuO nanoparticles have similar shapes without agglomeration. The nanoparticles of CuO with particle size

between 20-50 nm are seen inside TEM images. The XRD and TEM results confirm that the double-helical dinuclear copper(II) complexes $[\text{Cu}_2(\text{L}^1)_2]$ and $[\text{Cu}_2(\text{L}^2)_2]$ are suitable precursors for the preparation of CuO nanoparticles.

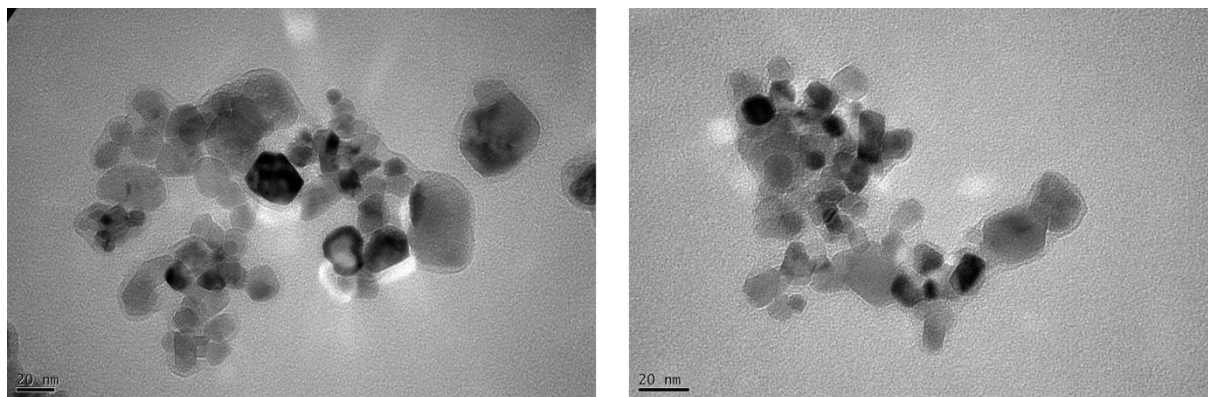


Fig. 6. TEM images of CuO nanoparticles prepared from $[\text{Cu}_2(\text{L}^1)_2]$ (left) and $[\text{Cu}_2(\text{L}^2)_2]$ (right)

4. Conclusion

The thermal properties of the bis-N,O-bidentate Schiff-base ligands and their double-helical dinuclear copper(II) complexes $[\text{Cu}_2(\text{L}^1)_2]$ and $[\text{Cu}_2(\text{L}^2)_2]$ have been investigated. We also examined the formation of CuO nanoparticles by solid-state thermal decomposition of $[\text{Cu}_2(\text{L}^1)_2]$ and $[\text{Cu}_2(\text{L}^2)_2]$, in an oven at 520°C. Pure and nanosized CuO nanoparticles with an average size between 10-30 nm have been successfully prepared.

References

- [1]. Ronson, T. K., Adams, H., Riis-Johannessen, T., Jeffery, J.C., Ward, M.D., *New J. Chem.* Vol. 30 (2006) pp. 26-28.
- [2]. Chu, Z., Huang, W., *J. Mol. Struct.* Vol. 837 (2007) pp. 15-22.
- [3]. Yoshida, N., Oshio, H., Ito, T., *J. Chem. Soc. Perkin Trans.* Vol. 2. (2001) pp. 1674-1678.
- [4]. Yoshida, N., Ito, T., Ichikawa, K., *J. Chem. Soc. Perkin Trans.* Vol. 2. (1997) pp. 2387-2392.
- [5]. Yoshida, N., Oshio, H., Ito, T., *J. Chem. Soc. Perkin Trans.* Vol. 2. (1999) pp. 975-983.
- [6]. Yoshida, N., Oshio, H., Ito, T., *Chem. Commun.* Vol. 2 (1998) pp. 63-64.
- [7]. Kondo, M., Shibuya, Y., Nabari, K., Miyazawa, M., Yasue, S., Maeda, K., Uchida, F., *Inorg. Chem. Commun.* Vol. 10 (2007) pp. 1311-1314.
- [8]. Wang, H., Zhang, D., Chen, Y., Ni, Z. H., Tian, L., Jiang, J., *Inorg. Chim. Acta.* Vol. 362 (2009) pp. 4972-4976.
- [9]. Albrecht, M., *Chem. Rev.* Vol. 101 (2001) pp. 3457-98.
- [10]. Alan, I., Kriza, A., Badea, M., Stanica, N., Olar, R., *J. Therm. Anal. Calorim.* Vol. 111 (2013) pp. 483-490.
- [11]. Taha, Z. A., Ajlouni, A., Al-Mustafa, J., *Chem. Pap.* Vol. 67 (2013) pp. 194-201.
- [12]. Oz, S., Kurtaran, R., Arici, C., Ergun, U., Dincer Kayay, F. N., Emregul, K. C., Atakol, O., *J. Therm. Anal. Calorim.* Vol. 99 (2010) pp. 363-368.
- [13]. Baran, Y., Kaya, I., Turkyilmaz, M., *J. Therm. Anal. Calorim.* Vol. 107 (2012) pp. 869-875.
- [14]. Bal, S., Bal, S. S., Erener, A., Halipci, H. N., Akar, S., *Chem. Pap.* Vol. 68 (2014) pp. 352-361.
- [15]. Kianfar, A. H., Kazemi Boudani, M., Roushani, M., Shamsipour, M., *J. Iran. Chem. Soc.* Vol. 9 (2012) pp. 449-453.
- [16]. Khalaji, A. D., Nikookar, M., Das, D., *J. Therm. Anal. Calorim.* Vol. 115 (2014) pp. 409-417.
- [17]. Khalaji, A. D., Das, D., *J. Therm. Anal. Calorim.* Vol. 114 (2013) pp. 671-675.
- [18]. Khalaji, A. D., Nikookar, M., Das, D., *Res. Chem. Intermed.* Vol. 41 (2015) pp. 357-363.

- [19]. Grivani, G., Tahmasebi, V., Khalaji, A. D., *Polyhedron*. Vol. 64 (2014) pp. 144-150.
- [20]. Khalaji, A. D., Nikookar, M., Charles, C., Triki, S., Thetiot, F., Das, D., *J. Clust. Sci.* Vol. 25 (2014) pp. 605-615.
- [21]. El-Trass, A., ElShamy, H., El-Mehasseb, I., El-Kemary, M., *App. Surface Sci.* Vol. 258 (2012) pp. 2997-3001.
- [22]. Chandrappa, K. G., Venkatesha, T. V., *J. Exp. Nanosci.* Vol. 8 (2013) pp. 516-532.
- [23]. Xu, H., Huang, J., Chen, Y., *Integ. Ferroelec.* Vol. 129 (2011) pp. 25-29.
- [24]. Li, S. Z., Zhang, H., Ji, Y. J., *Nanotech.* Vol. 15 (2004) pp. 1428-1435.
- [25]. Vidyasagar, C. C., Arthoba Naik, Y., Venkatesha, T. G., Viswanatha, R., *Nano-Micro. lett.* Vol. 4 (2012) pp. 73-77.
- [26]. Jia, X., Fan, H., Yang, W., *J. Dis. Sci. Tech.* Vol. 31 (2010) pp. 866-869.
- [27]. Wang, C., Li, Q., Wang, F., Xia, G., Liu, R., Li, D., Li, N., Spendelow, J. S., Wu, G., *ACS App. Mater. Interfaces.* Vol. 6 (2014) pp. 1243-1250.
- [28]. Sahoo, M., Sabbaghi, S., Saboori, R., *Mater. Lett.* Vol. 81 (2012) pp. 169-172.
- [29]. Mahato, T. H., Singh, B., Srivastava, A. K., Prasad, G. K., Srivastava, A. R., Ganesan, K., Vijayaraghavan, R., *J. Haz. Mater.* Vol. 192 (2011) pp. 1890-1895.